

Metal-Supported Niobium Catalysts Investigation for Conversion of Bio-Renewable Glycerol to Organic Compounds

Carolina F. M. Pestana,^a Bianca P. Pinto,^b Daniella R. Fernandes^a and Claudio J. A. Mota^b*,^{a,b,c}

^aInstituto de Química, Universidade Federal do Rio de Janeiro, Av. Athos da Silveira Ramos 149, CT Bl A, 21941-909 Rio de Janeiro-RJ, Brazil

^bEscola de Química, Universidade Federal do Rio de Janeiro, Av. Athos da Silveira Ramos 149, CT Bl E, 21941-909 Rio de Janeiro-RJ, Brazil

^cINCT Energia & Ambiente, Universidade Federal do Rio de Janeiro, 21941-909 Rio de Janeiro-RJ, Brazil

The glycerol oxidative dehydration to organic compounds, especially acrolein and acrylic acid, was studied over vanadium, molybdenum, and cobalt oxides supported on niobium oxide and niobium phosphate catalysts. At 300 °C, the glycerol conversion was 100% over all catalysts tested, and acrolein was the main product observed, without significant deactivation within the time on stream studied. Except for Co/V/Nb₂O₅, acrylic acid was formed over all catalysts, but the selectivity was not higher than 10%. Acetaldehyde and acetic acid were the other organic oxygenated products formed. Although the catalysts supported over Nb₂O₅ presented significantly lower acidity than the catalysts supported over NbOPO₄, they showed 100% glycerol conversion, indicating that the dehydration of glycerol does not require strong acidity. These data indicate the potential of niobium-based supports in the development of an active and selective catalyst for the glycerol oxidehydration to acrolein and acrylic acid, chemicals of great importance in the industry.

Keywords: acrolein, acrylic acid, dehydration, glycerol, niobium-base catalysts, oxidation

Introduction

Presently, a major part of the glycerol produced in the world comes from the transesterification of oils and fats for the production of biodiesel. In this process, approximately 100 kg of glycerol as a byproduct is inevitably generated when a ton of biodiesel is produced, causing a significant surplus of this product in recent years, due to the increase in the production of biofuel.¹ As a result, many efforts have been made to find new uses for the glycerol produced as a byproduct, especially as a renewable raw material for the chemical industry.²⁻⁴ Acid-catalyzed dehydration of glycerol is an excellent opportunity to produce high value-added chemicals, such as hydroxyacetone (acetol), acrolein, and acrylic acid. The major use of acrolein is in the production of acrylic acid,^{5,6} and acetol is mainly used as an intermediate for the production of other chemicals, such as

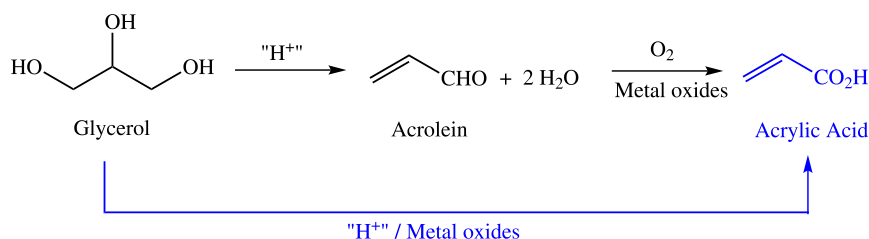
propylene glycol. It is also used to synthesize compounds such as propionaldehyde, acetone, and furan derivatives.⁷

The conversion of glycerol to acrylic acid may be carried out either in two steps, firstly involving the acid-catalyzed dehydration to acrolein and its subsequent oxidation to acrylic acid by the conventional V/Mo catalysts, or in a single step, involving the oxidehydration of glycerol over a bifunctional catalyst (containing acid and metallic functions) in the presence of air or oxygen (Scheme 1). This process has been receiving particular attention, because of the reduction of operational and capital expenditures compared with the two-step process.^{8,9} Nevertheless, the development of catalytic systems and reaction conditions for the one-step process is challenging, because dehydration is endothermic and favored at high temperatures, whereas oxidation of the formed acrolein is exothermic and difficult to be controlled at high temperatures, ultimately ending in CO₂.

Some studies on one-step glycerol oxidehydration have been reported. Wang *et al.*⁹ designed a catalyst featuring

*e-mail: cmota@iq.ufrj.br

Editor handled this article: Jaísa Fernandes Soares



Scheme 1. Glycerol routes to acrylic acid.

FeO_x domains embedded on the surface of a FeVO_4 phase, to evaluate its performance in the oxidative dehydration of glycerol. The best acrylic acid yield was 14% over the $\text{Fe}_{1.2}\text{V}$ catalyst. Soriano *et al.*¹⁰ reported the use of tungsten and vanadium mixed oxides for the same reaction. It was reported an ideal $\text{V}/(\text{W} + \text{V})$ ratio (0.12 to 0.21) for combining both the acid properties of tungsten oxide, which is an efficient catalyst for glycerol dehydration into acrolein in presence of oxygen, and the oxidizing properties of the vanadium ions. Chieragato *et al.*¹¹ also reported the use of tungsten and vanadium mixed oxides as catalysts for glycerol oxidehydration and found selectivity to acrylic acid of 25%. However, when niobium was incorporated in the structure, the acrylic acid selectivity was increased to 34%, showing a positive effect on the selectivity to acrolein and acrylic acid.

The glycerol oxidehydration to acrylic acid over vanadium impregnated zeolite was previously studied. The results were interpreted in terms of the vanadium dispersion inside the zeolite pores. For higher vanadium contents, the metal concentration on the outer zeolite surface increases, favoring the direct glycerol oxidation and preventing dehydration with the ultimate formation of acrylic acid.¹² Possato *et al.*¹³ reported an oxide-impregnated bifunctional zeolite catalyst for the glycerol oxidehydration, observing 97% of glycerol conversion and selectivity towards acrylic acid close to 17%, under air atmosphere. Other organic products were also observed, including acrolein and acetaldehyde. Although acrylic acid was produced on pure V_2O_5 , the glycerol conversion was low (5%), even at high temperatures (350 °C). In addition, high selectivity to acetic acid was observed.

Paula *et al.*¹⁴ synthesized vanadium silicates, isostructural to the titanium silicates ETS-10 and AM-6, which are active and selective for the glycerol oxidehydration to acrylic acid.¹⁴ The best performance was 94% of glycerol conversion and 86% selectivity to acrylic acid at 350 °C for 1 h of time stream in 100% O_2 atmosphere. However, when the reaction was carried out in 20% of O_2 , the glycerol conversion and acrylic acid selectivity decreased to 63 and 19%, respectively. Omata *et al.*¹⁵ studied a complex oxide of tungsten, vanadium, and niobium as a catalyst for the

direct oxidative transformation of glycerol to acrylic acid. It was observed 100% of glycerol conversion and 37% of acrylic acid selectivity. The acrylic acid selectivity was improved to 59% upon modification of the catalyst surface with 2.5 wt.% of phosphoric acid.

The gas phase glycerol conversion to acrylic acid over heteropoly acids was reported by Li and Zhang.¹⁶ The $\text{Cs}(\text{VO})_{0.2}(\text{PMo})_{0.25}(\text{PW})_{0.75}$ catalyst showed the best result, with 100% glycerol conversion and acrylic acid yield up to 60%, at 340 °C for 1 h of reaction. After 56 h of time on stream, the acrylic acid yield decreased to about 38%, showing good stability for coke deposition.

Martins and co-workers¹⁷ have studied the glycerol oxidehydration to acrylic acid.¹⁷⁻¹⁹ The authors evaluated the hydrothermal synthesis effects and heat-treatment in the formation of the crystalline phase of the vanadium and molybdenum mixed oxides. The catalysts treated under 100% oxidizing atmosphere showed the best catalytic performance to acrylic acid, achieving 33% selectivity at 320 °C. A gas flow rich in O_2 resulted in a suitable equilibrium in the phase formation of the mixed oxides containing V^{4+} and V^{5+} (MoVO_5 and $\text{Mo}_{4.65}\text{V}_{0.35}\text{O}_{14}$, respectively). Later, it was explored the influence of surfactants on the synthesis of molybdenum and vanadium mixed oxides for the glycerol oxidehydration.¹⁸ Both catalysts presented higher acrylic acid selectivity and good catalytic stability, with no coke formation and a considerable decrease in CO_x evolution during 6 h of reaction. Recently, Al-free vanadium silicates presenting structures analog to ferrierite and ITQ-6 zeolites were evaluated.¹⁹ [V]-ITQ-6(40) and [V]-FER(25) catalysts exhibit acrylic acid selectivity of 34 and 46%, respectively, presenting no significant deactivation after 6 h on stream. The authors reported that hydroxylated vanadium sites, formed by the dissociative adsorption of water, were responsible for extrinsic acidity and, consequently, glycerol dehydration.

In the present work, we wish to present results of glycerol oxidehydration over vanadium, molybdenum, and cobalt impregnated on niobium supports. To the best of our knowledge, there is no report of the use of these catalysts in this reaction. Compared to zeolites, niobium oxide and niobium phosphate are significantly less acidic,²⁰ which may impair the formation of excessive secondary products,

as well as catalyst deactivation. Besides, the use of niobium as catalyst support will contribute to the Brazilian economy since Brazil has a hegemony position about niobium, being the largest producer of this metal.

Experimental

Preparation of the catalysts

The supports of niobium oxide (Nb₂O₅) and niobium phosphate (NbOPO₄) were obtained from CBMM (Companhia Brasileira de Metalurgia e Mineração, Araxá, Brazil). Before the metal impregnation, the niobium oxide was calcined at 550 °C for 2 h under atmospheric air.

The catalysts were prepared by wet impregnation of the supports using ammonium metavanadate (NH₄VO₃), ammonium heptamolybdate tetrahydrate ((NH₄)₆Mo₇O₂₄·4H₂O) or cobalt nitrate hexahydrate (Co(NO₃)₂·6H₂O), all from Sigma-Aldrich, São Paulo, Brazil, analytical grade. Firstly, a given amount of the metallic salts (0.6 g of NH₄VO₃, 0.5 g of (NH₄)₆Mo₇O₂₄·4H₂O and 0.5 g of Co(NO₃)₂·6H₂O for Mo/V and Co/Mo niobium supported catalysts; 1.2 g of Co(NO₃)₂·6H₂O and 0.6 g of NH₄VO₃ for Co/V niobium supported catalyst) were dissolved in 70 mL of distilled water. Then, the support of niobium oxide or niobium phosphate (5 g) was added, and the system was kept under magnetic stirring at room temperature for 24 h. After this period, the water was carefully evaporated in a rotary evaporator to obtain the impregnated catalysts. After metal impregnation, the catalysts prepared by impregnation on niobium phosphate were calcinated in an oven at 550 °C for 2 h, whereas the catalysts prepared through the impregnation on niobium oxide were calcinated at 400 °C for 2 h. The final catalysts were named with the symbol of the impregnated metals and the molecular formula of the support. For instance, Co/V/NbOPO₄ stands for the catalysts impregnated with cobalt and vanadium oxide over niobium phosphate as support.

Characterization of materials

The chemical composition of the catalysts was analyzed by X-ray fluorescence (XRF) on a Philips PW 2400 spectrometer (Amsterdam, Netherlands) using a 3 KW Rh tube. The textural properties were analyzed by nitrogen adsorption at -196 °C on Micromeritics ASAP 2020 equipment (Norcross, United States). The surface area was determined using the Brunauer-Emmett-Teller (BET) method.

Powder X-ray diffraction (XRD) was obtained on a Shimadzu XRD 6000 X-ray diffractometer (Kyoto, Japan)

using Cu K α radiation operated at 40 kV and 30 mA. The X-ray patterns were collected in the 2 θ range of 5-80° (scan speed of 4 °C min⁻¹).

The total acidity and acid strength distribution of the supports and impregnated catalysts were estimated by temperature-programmed desorption of *n*-butylamine, following a procedure reported elsewhere.²¹

Catalysts tests

The catalytic tests were carried out in a continuous flow glass unit coupled online with a gas chromatograph to analyze the reaction products. A U-shaped glass reactor with a lateral stem was loaded with approximately 100 mg of catalyst to form a fixed bed. The catalyst was pre-treated under flowing nitrogen (40 mL min⁻¹) at 350 °C for 30 min. The reactor was then cooled to 300 °C and a 50 vol% glycerol aqueous solution was introduced at 0.5 mL h⁻¹ flow rate through the lateral stem with the aid of a syringe pump. In the oxidative dehydration studies, synthetic air (40 mL min⁻¹) was used as carrier gas instead of nitrogen.

The reactor effluent was analyzed by gas chromatography with flame ionization detector (Trace GC Ultra, Thermo Electron Corporation, Santa Clara, United States), using a column DB-225 (30 m, 0.25 mm, and 0.25 μ m) of (50%-cyanopropylphenyl)-dimethylpolysiloxane as stationary phase, to monitor the glycerol conversion and selectivity to the organic products. In control experiments, a sample of the gas phase was taken and analyzed on a gas chromatograph with a thermal conductivity detector, using Plot Q, a bonded polystyrene-divinylbenzene column (30 m, 0.320 mm, and 0.20 μ m).

The conversion of glycerol and product selectivity were calculated according to equations 1 and 2, respectively.

$$\text{Glycerol conversion} = \frac{\text{Moles of reacted glycerol}}{\text{Moles of initial glycerol}} \times 100 \quad (1)$$

$$\text{Product selectivity} = \frac{\text{Moles of obtained product}}{\text{Total moles of product}} \times 100 \quad (2)$$

Results and Discussion

The chemical and textural analyses of the catalysts and supports are shown in Table 1. The amount of metal obtained by chemical analysis coincides, satisfactorily, with the theoretical values added upon impregnation. The BET surface area decreases upon impregnation of the metals, with this behavior being more pronounced in the niobium phosphate catalysts. All the metal-supported niobium oxide

catalysts presented a similar BET surface area, whereas metal-supported niobium phosphate catalysts the BET surface values were ranged between 14 to 63 m² g⁻¹.

The acid sites of the samples were characterized by temperature-programmed desorption (TPD) using *n*-butylamine as a basic probe molecule. The TPD results of the catalysts and supports are shown in Table 2. Although this method does not give the exact acid strength of the materials, it allows a ready comparison of the acidity of different catalysts. The sites were classified of medium acid strength for desorption of the base within 120 to 350 °C, whereas strong acid sites were classified for desorption of the base in the range of 350 to 550 °C. The total acidity was taken from the whole range of desorption (120 to 550 °C). The niobium phosphate support shows a total acidity higher than the niobium oxide support. It also exhibits a significantly higher concentration of stronger acid sites. However, its acid strength is lower than niobium oxide support.

Upon metal impregnation, the total acidity of the catalysts decreased relative to the free supports. This may be partly explained by the textural characterization that results

in the reduction of the BET surface area and volume pore size, indicating significant pore blockage by the metals, and, by consequence, lower acidity.

The catalysts impregnated on niobium oxide showed a decrease in the ratio of strong to medium acid sites upon metal impregnation. This behavior was particularly evident on Mo/V/Nb₂O₅, which showed the best result for the acrylic acid formation. For the catalysts supported over niobium phosphate, the ratio of strong to medium acidity was not significantly affected, except for the Mo/V/NbOPO₄ that presented an important and remarkable increase with metal impregnation, probably the reason for the low acrylic acid formation.

Figures 1 and 2 show the XRD patterns of the catalysts and the calcined Nb₂O₅ and NbOPO₄ supports. Niobium oxide is amorphous before calcination but forms a crystalline structure after the thermal treatment process. The XRD pattern is consistent with the formation of the orthorhombic crystalline structure, which is usually formed when calcination is carried out above 500 °C.²² On the other hand, niobium phosphate did not show any appreciable change in crystallinity upon calcination.

Table 1. Chemical and textural characterization of the catalysts

Catalyst	XRF chemical composition / %				BET area / (m ² g ⁻¹)	Pore volume / (cm ³ g ⁻¹)
	P	V	Mo	Co		
Nb ₂ O ₅	–	–	–	–	40	0.117
Co/V/Nb ₂ O ₅	–	0.5	–	0.6	18	0.076
Mo/Co/Nb ₂ O ₅	–	–	0.4	0.7	24	0.087
Mo/V/Nb ₂ O ₅	–	0.6	0.3	–	25	0.083
NbOPO ₄	6.3	–	–	–	162	0.182
Co/V/NbOPO ₄	2.6	0.9	–	0.8	63	0.221
Mo/Co/NbOPO ₄	3.7	–	0.4	0.4	29	0.183
Mo/V/NbOPO ₄	2.6	0.9	0.4	–	14	0.063

XRF: X-ray fluorescence; BET: Brunauer-Emmett-Teller.

Table 2. Acidity by *n*-butylamine termodesorption

Catalyst	Acidity / (μmol g ⁻¹ NH ₃)			
	Medium ^a	Strong ^b	S/M ratio ^c	Total
Nb ₂ O ₅	98	74	0.76	172
Co/V/Nb ₂ O ₅	114	56	0.49	170
Mo/Co/Nb ₂ O ₅	51	24	0.47	75
Mo/V/Nb ₂ O ₅	60	9	0.15	69
NbOPO ₄	456	149	0.33	605
Co/V/NbOPO ₄	169	53	0.31	222
Mo/Co/NbOPO ₄	280	88	0.31	368
Mo/V/NbOPO ₄	91	48	0.53	139

^aAssociated with desorption of the base between 120 and 350 °C; ^bassociated with desorption of the base between 350 and 550 °C; ^cratio of strong to medium acidity.

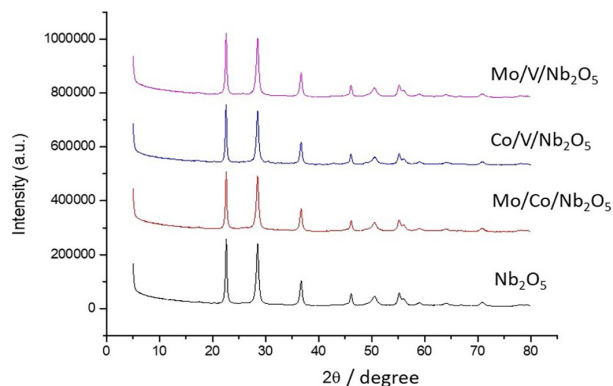


Figure 1. XRD patterns of metallic catalysts supported on Nb₂O₅.

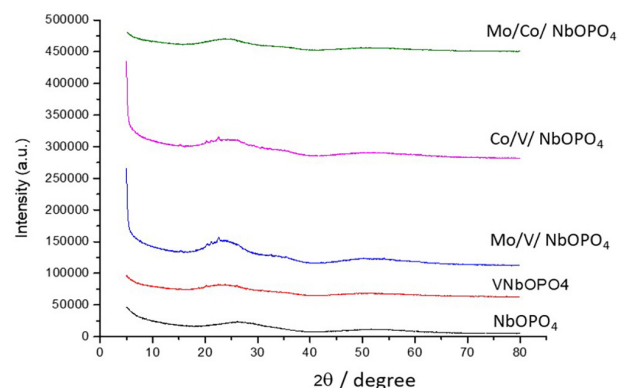


Figure 2. XRD patterns of metallic catalysts supported in NbOPO₄.

The results indicate that the crystalline phases of the niobium oxide-based catalysts are mostly identical to the free support, and no clear peak related to crystalline phases of the metal oxides could be observed. The absence of peaks related to the crystalline phase of the metal oxides suggests that the metal phases could be highly dispersed on the surface forming tiny particles, invisible to XRD diffraction. However, we cannot completely rule out the partial incorporation into the structure of the niobium support, forming solid solutions. Indeed, some literature studies on V₂O₅ and MoO₃ supported on Nb₂O₅ pointed out that the crystalline phase of vanadium oxide is only detected when the concentration of the metal is above 15 wt.%, whereas the crystalline phase of MoO₃ can be observed for concentrations above 5 wt%.²³

It is known that niobium phosphate is an amorphous material and becomes crystalline only after heating above 800 °C.²⁴ This characteristic is maintained after the metal impregnation. In this work, the metal-impregnated niobium phosphate catalysts were calcined at 550 °C and no crystalline phases, either of the metal oxides or the support, could be identified. It has been reported that the crystalline V₂O₅ phase supported on niobium phosphate is only visible when the vanadium content is 25 wt.%. No diffraction peaks were observed for values of vanadium

between 5 and 15 wt.%, due to the high dispersion of the metal over the surface of the support.²⁵

The catalytic tests were performed within 450 min on stream. All catalysts were active for glycerol oxidehydration. It was reported that catalysts for the dehydration of glycerol to acrolein and oxidehydration of glycerol produce coke and deactivate in a matter of hours.²⁶ The transient activation of the catalysts has been recognized in many catalysts, showing that selectivity to acrolein is increasing over time. However, no significant deactivation was observed within this period.

Table 3 shows the results of glycerol conversion and product selectivity to organic compounds over niobium oxide and niobium phosphate supports under N₂ flow at 300 °C. In both catalysts, acrolein was the main product, indicating that these acidic supports are good catalysts for glycerol dehydration, showing 100% conversion under the reaction conditions used in the experiments. Other observed organic products were acetaldehyde, formaldehyde, and acetol. This last product was only formed over niobium phosphate. Acetaldehyde is probably formed by the cracking of the 3-hydroxypropanal intermediate, whereas acetic acid can be produced by oxidation of the formed acetaldehyde.

Table 3. Glycerol dehydration over niobium-based supports

Support	Nb ₂ O ₅	NbOPO ₄
Conversion / %	100	100
Selectivity / %		
Acrolein	74	80
Acetaldehyde	20	5
Formaldehyde	6	3
Hydroxyacetone	–	12

Reaction conditions: 100 mg of catalyst, 50 vol% glycerol aqueous solution, 0.5 mL h⁻¹ N₂ flow rate, at 300 °C, 450 min.

Figures 3 and 4 show the conversion and selectivity to organic compounds of the glycerol oxidehydration over metal-impregnated Nb₂O₅ and NbOPO₄ catalysts, respectively. The conversion was 100% for all catalysts, indicating that the acidity of the materials was enough to catalyze the dehydration of the glycerol molecule. This fact reinforces the hypothesis that, under these conditions, the reaction does not require catalysts of high acidity, as those observed for metal-free supports. Indeed, it seems that sites of medium acid strength play an important role in the catalytic glycerol oxidehydration to acrylic acid. For instance, the Mo/V/Nb₂O₅ catalyst presented the lowest amount of strong acid sites (9 μmol g⁻¹ NH₃) and total acidity (69 μmol g⁻¹ NH₃), but the same conversion as the

other catalysts. In addition, the selectivity to acrylic acid was one of the highest, with a value of 10%, over the same catalyst. The tuning of the acid strength is important to prevent undesired secondary reactions. Zeolites and other strong acids, for example, catalyze many side reactions, decreasing the selectivity to acrolein.²⁷

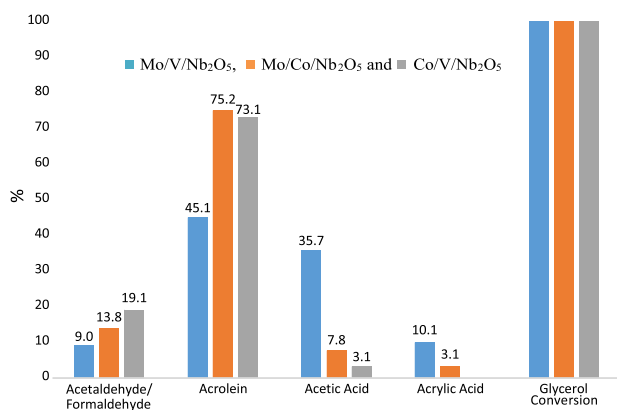


Figure 3. Conversion and selectivity to organic products of the glycerol oxidative dehydration over metallic catalysts supported on Nb₂O₅. Reaction conditions: 100 mg of catalyst, 50 vol% glycerol aqueous solution, 0.5 mL h⁻¹ air flow rate, at 300 °C, 450 min.

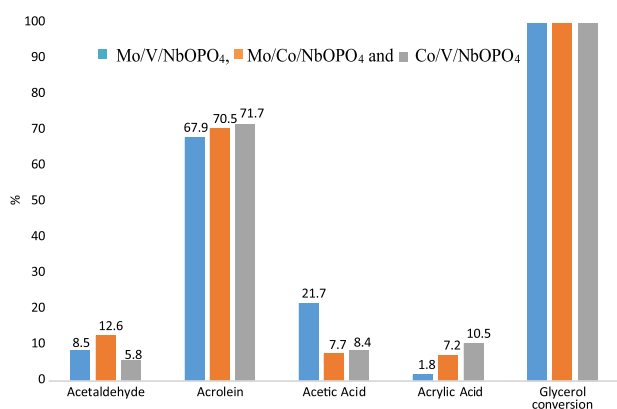


Figure 4. Conversion and selectivity to organic products of the glycerol oxidative dehydration over metallic catalysts supported on NbOPO₄. Reaction conditions: 100 mg of catalyst, 50 vol% glycerol aqueous solution, 0.5 mL h⁻¹ air flow rate, at 300 °C, 450 min.

All catalysts showed mostly the same products, with acrolein being the major one on all of them. These results suggest that the acidity of the catalytic system is well-tuned for glycerol dehydration to acrolein. The acrylic acid, which is another organic compound of great industrial interest, presented a selectivity of 10% in most of the tested catalysts, implying that the catalyst studied were active for the oxidation of acrolein to acrylic acid. Therefore, this study indicates a great potential of application for this metal-impregnated niobium catalyst system.

The only catalyst that did not produce acrylic acid under the conditions chosen in this work was the Co/V/Nb₂O₅

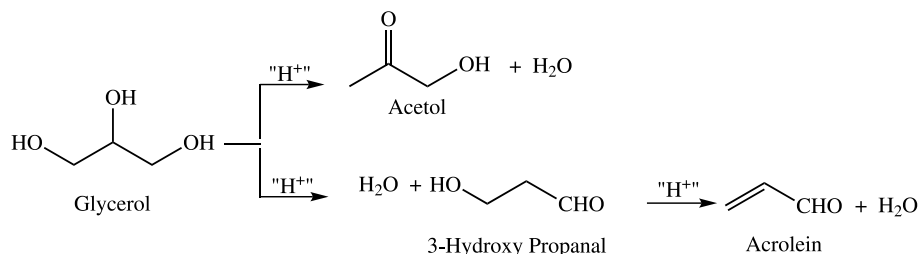
(Figure 3). This catalyst presented total acidity similar to the support alone and half of its BET area value. Nevertheless, the same metallic system supported over niobium phosphate gave the highest selectivity to acrylic acid (10.5%) among the catalysts tested. Considering the same support, the acrylic acid selectivity seems to be related to the BET surface area, pore volume size, and acidity strength, but not with the composition of the metallic phase.

Although V and Mo oxides are traditional components of oxidation catalysts, cobalt has been reported to be a promoter in the oxidation of propene to acrolein over metal oxide catalysts, leading to higher conversion and acrolein yield.²⁸ In addition, it has also been reported²⁹ that Co and Mo oxides can be used together as an efficient catalytic system for the vapor phase oxidation of acrolein to acrylic acid.

These data support the hypothesis that the main reason for the poor selectivity to acrylic acid is related to the optimization of the metallic function and accordingly, the nature of surface sites, which also depend on the properties of the support. Therefore, by modifying the properties of the support, the reactivity of the metallic phase may also change. The main challenge is the optimization of the metal oxide loading without promoting extensive oxidation of the glycerol molecule to other products, as well as complete oxidation to form CO₂ and CO.

It is interesting to note that hydroxyacetone was not observed over the impregnated catalysts, but it was formed over pure NbOPO₄. This might imply that the reduction of the total acidity, especially the strong acid sites, affects the selectivity of glycerol dehydration. Hydroxyacetone is the product of dehydration of the primary hydroxyl of glycerol (Scheme 2). Previous literature results indicate that Lewis acidity is of prime importance for the formation of hydroxyacetone.^{30,31} Nevertheless, *in situ* infrared measurements³² revealed that, although the Lewis acid sites of Nb₂O₅ are involved in the dehydration of the primary hydroxyl of the glycerol molecule, the formed enol intermediate, 2-propene-1,2-diol, is stabilized on the catalyst surface and do not straightforwardly tautomerize to hydroxyacetone. On the other hand, dehydration of the secondary hydroxyl forms the enol intermediate 1,3-propenediol, which is not spectroscopically observed on the Nb₂O₅ surface and may desorb as 3-hydroxypropanal, which in turn may be further dehydrated to acrolein. These considerations may explain the results.

The NbOPO₄ support has almost twice the number of strong acid sites than Nb₂O₅ (149 μmol g⁻¹ for NbOPO₄ and 74 μmol g⁻¹ for Nb₂O₅), and the total acidity is more than three times higher (605 μmol g⁻¹ for NbOPO₄ and 172 μmol g⁻¹ for Nb₂O₅). It has also been reported that



Scheme 2. Acid-catalyzed dehydration of glycerol; formation of acetol upon dehydration of the primary hydroxyl or formation of 3-hydroxy propanal upon dehydration of the secondary hydroxyl.

niobium phosphate possesses more Brønsted than Lewis acid sites, whereas on niobium oxide Lewis acidity prevails when the solid is calcined at 300 °C.³³ But this profile changes with increasing pretreatment temperature, due to the transformation of the protonic acid sites in Lewis acid sites by water elimination and loss of surface area.³⁴

In a previous study,¹² using vanadium-impregnated zeolite Beta, the selectivity to acrylic acid was around 25% with a glycerol conversion of 70% at 275 °C. Other studies⁸⁻¹⁰ on the use of bifunctional catalysts report selectivity to acrylic acid in the range of 5 to 30%, at different reaction conditions and conversion levels. On the other hand, massic mixed oxides of tungsten, vanadium, and niobium gave 50% selectivity to acrylic acid at 100% glycerol conversion.³⁵ The selectivity to acrolein is, however, rather low, in the range of 3%, with the formation of CO and CO₂, as well as other heavier products.

In this work, although CO and CO₂ formed during the tests have not been measured online, it was possible to quantify the CO and CO₂ content, in control experiments where a sample of the reactor effluent was collected and analyzed in a thermal conductivity detector (TCD) gas chromatograph. The results indicated that about 18% of the glycerol is transformed in CO₂ over Mo/V/Nb₂O₅ catalyst in the same reaction conditions used in this work. Therefore, considering the mass balance and taking into account the formed inorganic gaseous products (CO and CO₂), the corrected selectivity to acrolein plus acrylic acid (A + AA) could be obtained for this catalyst. Table 4 shows a comparison of the reported selectivity to acrolein and acrylic acid with other studies, where the amount of CO and CO₂ formed was reported.

It is possible to observe that Mo/V/Nb₂O₅ catalyst shows 60% of selectivity to acrolein plus acrylic acid. Massic mixed oxides, although producing higher amounts of acrylic acid, gave lower selectivity to acrolein plus acrylic acid, consistent with the high activity of these catalysts to the complete oxidation of the organic compounds to CO and CO₂.^{35,36} Vanadium phosphate showed the highest selectivity to acrolein plus acrylic acid, around 69%, at 300 °C, with only 1% of CO₂.³⁷ Nevertheless, this value

Table 4. Conversion and selectivity to acrolein plus acrylic acid of the glycerol oxidehydration over different catalytic systems and conditions

Catalyst	Conversion / %	Selectivity / %		Reference
		A + AA	CO _x	
V-W-Nb oxides	100	53	30	13
VOHPO ₄ ^a	100	69	1	36
VOHPO ₄ ^b	100	44	22	36
Mo-V-Te-Nb oxides	100	30	45	37
V ₂ O ₅ /ZSM-5	100	32	60	38
Mo/V/Nb ₂ O ₅	100	60	18	this work

^aResults at 300 °C; ^bresults at 350 °C; A + AA corresponding to acrolein plus acrylic acid.

mostly accounts for acrolein (66%), with acrylic acid being formed in only 3%. When the temperature was increased to 350 °C, the selectivity to acrylic acid was 8%, but the selectivity to acrolein decreased to 36%, whilst the amount of CO and CO₂ accounted for 22%. These results indicate the potential of the metal oxide systems supported over Nb₂O₅ as catalysts for the oxidehydration of glycerol to acrolein and acrylic acid. The main advantage is the low formation of byproducts, especially heavier ones, with high selectivity to the desired products. Therefore, the acidic properties of niobium-based catalysts appear to be well suited for the dehydration of glycerol to acrolein. By evaluating the function of metal oxides, it was possible to observe their ability to oxidize acrolein to acrylic acid by up to 10%. This result indicates a great potential of these bifunctional catalysts to produce acrylic acid in a single step, from glycerol oxidehydration.

Conclusions

The oxidative dehydration of glycerol to organic compounds such as acrolein and acrylic acid over metal-impregnated niobium oxide and niobium phosphate catalysts was studied. Although the acidity of the supports was significantly reduced upon metal impregnation, all tested materials presented 100% conversion. These results indicate that the glycerol dehydration to acrolein does not

require strong acid sites at the conditions used in this study and that the niobium-based supports are well adjusted, in terms of acidity, to catalyze this reaction.

The main organic product in all catalysts was acrolein, with selectivity ranging from 50 to 70%, approximately. Acrylic acid was produced in up 10% selectivity, with the remaining products being acetaldehyde/formaldehyde and acetic acid. All catalysts did not show significant deactivation during 450 min on stream, indicating that either the formed coke is burned at the reaction conditions or the acid function was well adjusted to prevent coke deposition.

Although the niobium supports appear to have the suitable acidity (number and strength) to dehydrate glycerol to acrolein, the metal oxide function still deserves attention to improve the selectivity to acrylic acid without increasing the amount of CO and CO₂. Over the Mo/V/Nb₂O₅ catalyst, the selectivity to acrolein plus acrylic acid, both products of great industrial relevance, are among the highest reported in the literature, indicating that the formation of undesired byproducts is not much significant over the catalytic system studied, which points out for the potential sustainability of the process.

Acknowledgments

Authors thank FAPERJ, CNPq, PRH-ANP, and FINEP for financial support.

References

- Pinto, A. C.; Guarieiro, L. L. N.; Rezende, M. J. C.; Ribeiro, N. M.; Torres, E. A.; Lopes, W. A.; Pereira, P. A. P.; de Andrade, J. B.; *J. Braz. Chem. Soc.* **2005**, *16*, 1313.
- Mota, C. J. A.; Pinto, B. P.; de Lima, A. L.; *Glycerol: A Versatile Renewable Feedstock for the Chemical Industry*; Springer: Cham, Switzerland, 2017.
- Behr, A.; Eilting, J.; Irawadi, K.; Leschinski, J.; Lindner, F.; *Green Chem.* **2008**, *10*, 13.
- Mota, C. J. A.; Silva, C. X. A. D.; Gonçalves, V. L. C.; *Quim. Nova* **2009**, *32*, 639.
- Andrushkevich, T. V.; *Catal. Rev.* **1993**, *35*, 213.
- Kampe, P.; Giebeler, L.; Samuelis, D.; Kunert, J.; Drochner, A.; Haaß, F.; Adams, A. H.; Ott, J.; Endres, S.; Schimanke, G.; Buhrmester, T.; Martin, M.; Fuess, H.; Vogel, H.; *Phys. Chem. Chem. Phys.* **2007**, *9*, 3577.
- Mohamad, M. H.; Awang, R.; Yunus, W. M. Z. W.; *Am. J. Appl. Sci.* **2011**, *8*, 1135.
- Wang, F.; Dubois, J. L.; Ueda, W.; *Appl. Catal., A* **2010**, *376*, 25.
- Wang, F.; Xu, J.; Dubois, J. L.; Ueda, W.; *ChemSusChem* **2010**, *3*, 1383.
- Soriano, M. D.; Concepción, P.; Nieto, J. M. L.; Cavani, F.; Guidetti, S.; Trevisanut, C.; *Green Chem.* **2011**, *13*, 2954.
- Chierigato, A.; Basile, F.; Concepción, P.; Guidetti, S.; Liosi, G.; Soriano, M. D.; Trevisanut, C.; Cavani, F.; Nieto, J. M. L.; *Catal. Today* **2012**, *197*, 58.
- Pestana, C. F. M.; Guerra, A. C. O.; Ferreira, G. B.; Turci, C. C.; Mota, C. J. A.; *J. Braz. Chem. Soc.* **2013**, *24*, 100.
- Possato, L. G.; Cassinelli, W. H.; Garetto, T.; Pulcinelli, S. H.; Santilli, C. V.; Martins, L.; *Appl. Catal., A* **2015**, *492*, 243.
- Paula, A. S.; Possato, L. G.; Ratero, D. R.; Contro, J.; Keinan-Adamsky, K.; Soares, R. R.; Goobes, G.; Martins, L.; Nery, J. G.; *Microporous Mesoporous Mater.* **2016**, *232*, 151.
- Omata, K.; Matsumoto, K.; Murayama, T.; Ueda, W.; *Catal. Today* **2016**, *259*, 205.
- Li, X.; Zhang, Y.; *ACS Catal.* **2016**, *6*, 2785.
- Rasteiro, L. F.; Vieira, L. H.; Possato, L. G.; Pulcinelli, S. H.; Santilli, C. V.; Martins, L.; *Catal. Today* **2017**, *296*, 10.
- Rasteiro, L. F.; Vieira, L. H.; Santilli, C. V.; Martins, L.; *RSC Adv.* **2018**, *8*, 11975.
- Vieira, L. H.; Lopez-Castillo, A.; Jones, C. W.; Martins, L.; *Appl. Catal., A* **2020**, *602*, 117687.
- Gonçalves, V. L. C.; Rodrigues, R. C.; Lorençato, R.; Mota, C. J. A.; *J. Catal.* **2007**, *248*, 158.
- Gonçalves, V. L. C.; Pinto, B. P.; Silva, J. C.; Mota, C. J. A.; *Catal. Today* **2008**, *133-135*, 673.
- Eblagon, K. M.; Malaika, A.; Ptaszynska, K.; Pereira, M. F. R.; Figueiredo, J. L.; *Nanomaterials* **2020**, *10*, 1685.
- Jehng, J. M.; Turek, A. M.; Wachs, I. E.; *Appl. Catal., A* **1992**, *83*, 179.
- Tang, Z. C.; Yu, D. H.; Sun, P.; Li, H.; Huang, H.; *Bull. Korean Chem. Soc.* **2010**, *31*, 3679.
- Sun, Q.; Fang, D.; Wang, S.; Shen, J.; Auroux, A.; *Appl. Catal., A* **2007**, *327*, 218.
- Dalil, M.; Carnevali, D.; Edake, M.; Auroux, A.; Dubois, J. L.; Patience, G. S.; *J. Mol. Catal. A: Chem.* **2016**, *421*, 146.
- Chai, S. H.; Wang, H. P.; Liang, Y.; Xu, B. Q.; *Green Chem.* **2007**, *9*, 1130.
- Udalova, O. V.; Shashkin, D. P.; Shibanova, M. D.; Krylov, O. V.; *Kinet. Catal.* **2005**, *46*, 569.
- Campos, D.; Hecquet, G.; Pham, C.; *US pat. 006310240B1*, **2001**.
- Katryniok, B.; Paul, S.; Bellière-Baca, V.; Rey, P.; Dumeignil, F.; *Green Chem.* **2010**, *12*, 2079.
- Belousov, A. S.; *ChemistrySelect* **2021**, *6*, 9191.
- Foo, G. S.; Wei, D.; Sholl, D. S.; Sievers, C.; *ACS Catal.* **2014**, *4*, 3180.
- Bassan, I. A. L.; Nascimento, D. R.; San Gil, R. A. S.; da Silva, M. I. P.; Moreira, C. R.; Gonzalez, W. A.; Faro, A. C.; Onfroy, T.; Lachter, E. R.; *Fuel Process. Technol.* **2013**, *106*, 619.
- Nowak, I.; Ziolk, M.; *Chem. Rev.* **1999**, *99*, 3603.

35. Chieregato, A.; Soriano, M. D.; Basile, F.; Liosi, G.; Zamora, S.; Concepción, P.; Cavani, F.; López Nieto, J. M.; *Appl. Catal., B* **2014**, *150-151*, 37.
36. Doornkamp, C.; Ponec, V.; *J. Mol. Catal. A: Chem.* **2000**, *162*, 19.
37. Possato, L. G.; Diniz, R. N.; Garetto, T.; Pulcinelli, S. H.; Santilli, C. V.; Martins, L.; *J. Catal.* **2013**, *300*, 102.
38. Wang, F.; Dubois, J. L.; Ueda, W.; *J. Catal.* **2009**, *268*, 260.

Submitted: September 10, 2021

Published online: February 22, 2022

